ChemComm

Check for updates

Bimodal detection of carbon dioxide using fluorescent molecular aggregates†

Rakesh K. Mishra, [ID] *[ab] Samiyappan Vijayakumar, [ID] [a] Arindam Mal, [ID] [ac]
Varsha Karunakaran, [ID] [cd] Jith C. Janardhanan, [ID] [a] Kaustabh Kumar Maiti, [ID] [cd]
Vakayil K. Praveen [ID] *[ac] and Ayyappanpillai Ajayaghosh [ID] *[ac]

Cyano-substituted *p*-phenylenevinylene (R-1) aggregates exhibiting fluorescence and Raman spectroscopic responses towards CO_2 are described. The aggregation-induced emission (AIE) as well as the aggregation-enhanced Raman scattering (AERS) of R-1 in aqueous conditions was reduced in the presence of a small amount of CO_2, which enabled its easy and fast bimodal detection in different analytical samples.

The capture, storage, release and conversion of CO_2 are issues of high priority research.[1,2] In this context, the easy and fast detection of CO_2 is an important objective. Hence, researchers are looking for simple and effective sensors/receptors for CO_2.[3–5] For this purpose, optical detection based on self-assembled fluorescent molecules is considered to be viable owing to its high sensitivity, fast response time, low cost, visual signal transduction, real-time *in situ* responses, and compatibility for *in vivo* analysis.[3] A possible approach to realize such sensors depends on the analyte-triggered self-assembly or disassembly of a given molecular probe, producing a turn-on/off fluorescence response.[6] Moreover, the combination of more than one detection modality is preferred in order to increase the selectivity and sensitivity of the probe.[3,6] For instance, fluorescent probes that are Raman-active can be used as bimodal sensors.[7] This is particularly relevant considering the fact that many of the reported CO_2 sensors rely on single detection modality and often utilize more than one receptor components.[5]
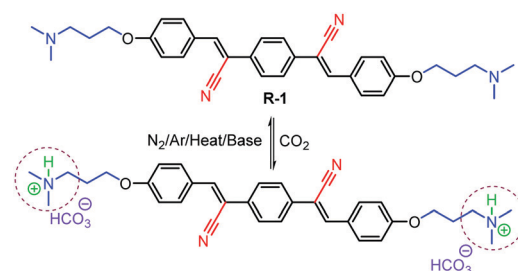
Scheme 1   Receptor **R-1** and its interaction with CO_2.

Herein, we report the fluorescence as well as Raman-assisted sensing of CO_2 using a cyano-substituted[8] *p*-phenylenevinylene[9] molecule bearing terminal tertiary amine moieties (Scheme 1). The receptor **R-1** was synthesized as per Scheme S1 (ESI†). All intermediates and final compounds obtained were characterized using FT-IR, ^{1}H, and ^{13}C NMR techniques and mass spectrometry (Fig. S1–S8, ESI†).

The receptor **R-1** was highly soluble in THF and DMSO and formed aggregates (**R-1**$_{Agg}$) in an aqueous medium, as indicated by the observed Tyndall effect (Fig. 1a, inset). The UV/Vis spectrum of **R-1**$_{Agg}$ (1×10^{-4} M) in the aqueous medium shows a narrow blue-shifted band (λ_{max} = 348 nm) in comparison to the broad spectrum in DMSO (λ_{max} = 375 nm), where it mainly exists as molecularly dissolved species (Fig. 1a). The aggregation of **R-1** was also marked by the origin of an intense yellow emission (λ_{em} = 550 nm) owing to the AIE properties of the chromophoric unit (Fig. 1b, inset).[10] On the contrary, the **R-1** monomer in DMSO displayed a blue-shifted weak emission at 465 nm, τ = 5.84 ps (Fig. S9a and Table S1, ESI†). The red-shift and structureless features of emission in aqueous conditions indicated the formation of excimer-like species on aggregation, as evident from the longer average lifetime value (τ = 5.67 ns).[11] Systematic aggregation studies were carried out in a DMSO-water mixture using UV/Vis and fluorescence spectroscopies, revealing that **R-1** starts to aggregate in a 70 : 30 water–DMSO mixture. The maximum fluorescence intensity was observed in a 99 : 1

[a] Photosciences and Photonics Section, Chemical Sciences and Technology Division, CSIR-National Institute for Interdisciplinary Science and Technology (CSIR-NIIST), Thiruvananthapuram – 695019, India. E-mail: vkpraveen@niist.res.in, aajayaghosh@niist.res.in

[b] Department of Sciences and Humanities, National Institute of Technology, Uttarakhand (NITUK), Srinagar (Garhwal) – 246174, India. E-mail: rkmishra@nit.uk.ac.in

[c] Academy of Scientific and Innovative Research (AcSIR), Ghaziabad – 201002, India

[d] Organic Chemistry Section, Chemical Sciences and Technology Division, CSIR-NIIST, Thiruvananthapuram – 695019, India

† Electronic supplementary information (ESI) available: Experimental details, synthesis procedures and characterization data of the compounds, and additional figures. See DOI: 10.1039/c9cc01564g
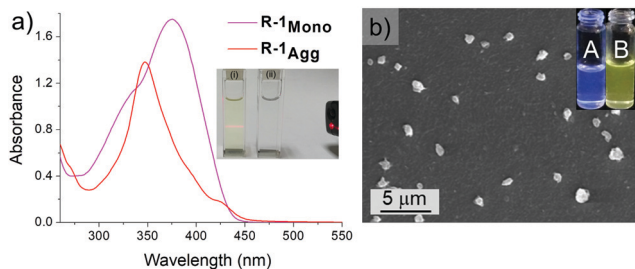
Fig. 1 (a) Absorption spectra of **R-1** (1×10^{-4} M) in DMSO and an aqueous medium (water/DMSO, 99/1 v/v). Inset shows the images of the Tyndall effect of the corresponding solutions, indicating the aggregation behaviour of **R-1** in aqueous medium (i). (b) SEM image of **R-1$_{agg}$** (1×10^{-4} M, water/DMSO, 99/1 v/v) drop cast over a silicon wafer. Inset shows the change in the fluorescence of **R-1** in DMSO (A) and in a 99 : 1 water/DMSO mixture (B). Images were taken under 365 nm UV light illumination.

water–DMSO mixture (Fig. S9 (ESI†) and Fig. 1b, inset). The scanning electron microscopy (SEM) images of a drop cast sample of **R-1$_{Agg}$** (1×10^{-4} M, water/DMSO, 99/1 v/v) over a silicon wafer show particle-like morphology (Fig. 1b).

Having these results in hand, we tested the CO_2 sensing ability of **R-1$_{Agg}$** (1×10^{-4} M, water/DMSO, 99/1 v/v) on purging CO_2 into **R-1$_{Agg}$** while monitoring the corresponding changes in its absorption and emission properties. It was observed that in the presence of CO_2, the sharp absorption band at 348 nm of **R-1$_{Agg}$** broadened and red-shifted to 364 nm (Fig. 2a). Interestingly, gradual quenching in the emission of **R-1$_{Agg}$** was observed on purging of CO_2 (Fig. 2b and Fig. S10, ESI†). Fluorescence titration experiments revealed that the yellow emission of the aggregates
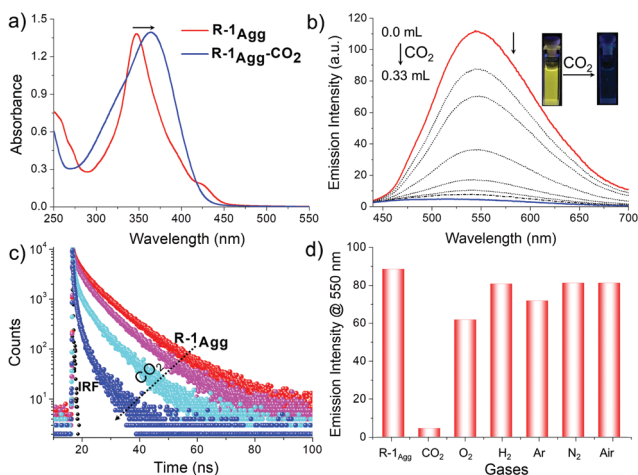

Fig. 2 (a) Absorption spectra of **R-1$_{Agg}$** (1×10^{-4} M) in aqueous medium (water/DMSO, 99/1 v/v) after purging with excess amount of CO_2 (0.33 mL). (b) Emission spectra of **R-1$_{Agg}$** (1×10^{-4} M, λ_{ex} = 370 nm) in the presence of different concentrations of CO_2 (0, 0.016, 0.032, 0.048, 0.064, 0.080, 0.096, and 0.33 mL). Inset shows the fluorescence change of **R-1$_{Agg}$** under UV illumination (λ_{ex} = 365 nm) before and after purging with CO_2. (c) Fluorescence lifetime decay profile of **R-1$_{Agg}$** (λ_{ex} = 370 nm, λ_{em} = 550 nm) in the presence of increasing CO_2 concentrations (0, 0.016, 0.048 and 0.33 mL). IRF = instrument response function. (d) Fluorescence response (λ_{ex} = 370 nm) of **R-1$_{Agg}$** towards CO_2 after purging with different gases (3.0 mL) in aqueous medium; from left to right: **R-1$_{Agg}$**, CO_2, O_2, H_2, Ar, N_2 and air.

reduced by 25-fold with 0.33 mL of CO_2. Fig. 2c shows the fluorescence decay profiles of **R-1$_{Agg}$** (probed at 550 nm) on purging with CO_2. **R-1$_{Agg}$** exhibited a triexponential decay with an average lifetime of 5.67 ns, whereas in the presence of CO_2, a faster decay with an average lifetime of 0.33 ns was observed (Table S1, ESI†). The changes in absorption, steady state and time-resolved emission characteristics indicated the transformation of **R-1$_{Agg}$** into a new-type of species having monomer-like absorption and emission features.

This observation was also supported by dynamic light scattering (DLS) studies. The average particle diameter of **R-1$_{Agg}$** (1×10^{-4} M) as measured by DLS was found to be 156 ± 10 nm. On purging a small amount of CO_2, the size of the aggregates gradually decreased; this was inferred from the reduction in the average particle diameter to 102 ± 10 nm, which was further reduced to 83 ± 5 nm with excess (0.33 mL) of CO_2 (Fig. S11, ESI†). Furthermore, a reduction in the Tyndall effect of **R-1$_{Agg}$** in the presence of CO_2 (0.33 mL) was also noticed (Fig. S11c, ESI†). The results of the fluorescence titration studies, size distribution, Tyndall effect and CO_2 chemistry with amine moieties in an aqueous medium suggested that **R-1$_{Agg}$** was protonated in the presence of CO_2 gas, leading to a change in the molecular character from hydrophobic to hydrophilic (Scheme 1). Thus, the large **R-1$_{Agg}$** was converted into a mixture of mono-mers and smaller aggregates of the positively charged **R-1**.[12] These processes were indicated by the simultaneous red shift of the absorption maximum and the reduction in the AIE property of the fluorophores; this was corroborated by the pH-dependent fluorescence titration studies (Table S2 and Fig. S12, ESI†), yielding a pK_a value for **R-1** as 6.98 (±0.007).

To further evaluate the selectivity of **R-1$_{Agg}$** towards CO_2, we carried out fluorescence titration experiments with different gases in excess amounts (3.0 mL) including N_2, O_2, Ar, H_2, and air under identical conditions (Fig. 2d). It was clearly observed that CO_2 produced the most significant effect on the fluorescence properties of **R-1$_{Agg}$**. The experimental results also indicated that the detection of CO_2 using **R-1$_{Agg}$** experiences less interference from other common gases present in air. In addition, the binding of CO_2 to **R-1$_{Agg}$** was found to be reversible (Scheme 1). The less emissive **R-1$_{Agg}$**–CO_2 adduct was readily converted back into highly fluorescent **R-1$_{Agg}$** by purging N_2/Ar or by adding a small amount of K_2CO_3 at room temperature. As shown in Fig. S13 (ESI†), on repeated purging of CO_2 and addition of 0.1 mM K_2CO_3 solution, the emission of **R-1$_{Agg}$** exhibits multiple cycles of reversible on–off changes.

Fluorescence microscopy imaging was carried out to explore the capability of **R-1$_{Agg}$** as a probe for monitoring the variation of external CO_2 concentration inside living cells. For this purpose, lung adenocarcinoma cells A549 were incubated with 100 μM of **R-1$_{Agg}$** for 1 h under normal atmospheric conditions (0.038% CO_2) at 25 °C as we observed that the above-mentioned concentration gave optimum fluorescence intensity with minimal cytotoxicity around 3 h (Fig. S14, ESI†). Also, initial localization of **R-1$_{Agg}$** was observed inside the nucleus in 1 h (Fig. S15, ESI†), but it eventually spread throughout the cells. As shown in Fig. 3, a yellow fluorescence signal can be observed, confirming the internalization of the aggregates inside the intercellular milieu.
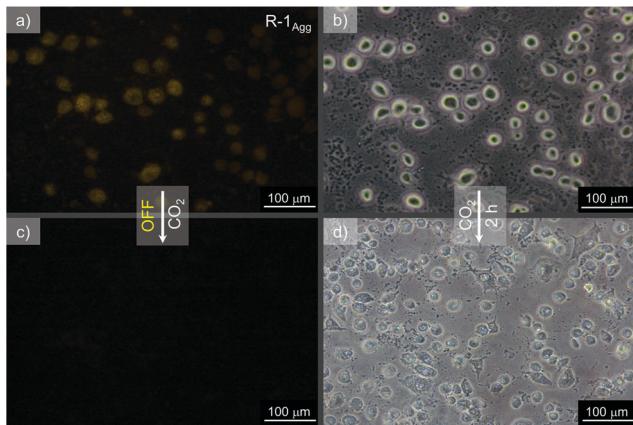
Fig. 3 (a) Fluorescence and (b) bright field images of **R-1**$_{Agg}$ in A549 lung cancer cells incubated with 100 μM **R-1**$_{Agg}$. (c) Fluorescence image of A549 cells further incubated for 2 h at 25 °C and 5% CO_2 and (d) the corresponding bright field image.

Thereafter, the cells were kept in an incubation chamber with 5% CO_2 for 2 h, and the fluorescence was monitored against time. The emission intensity of the yellow fluorescence was reduced and almost no fluorescence was observed, while the sample cells kept under ambient conditions still showed the corresponding emission (Fig. S16, ESI†). These observations suggest that the increase in external CO_2 concentration causes a reduction in the fluorescence emission intensity, thus revealing the capability of **R-1**$_{Agg}$ to detect CO_2 variations in cellular conditions. Even though **R-1** showed slight toxicity after a higher incubation time, the probe could efficiently sense CO_2 inside the cellular environment.

The aggregation-enhanced Raman scattering (AERS) of **R-1**$_{Agg}$ was exploited as an additional modality for chemosensing purposes.[7,13] First, the Raman spectrum of **R-1**$_{Agg}$ (4×10^{-4} M, water/THF, 99/1 v/v) was recorded with a Raman microscope using 633 nm laser excitation.[13] The spectra were obtained using a CCD detector with an integration time of 0.5 s and 10 accumulations. A tiny droplet of **R-1**$_{Agg}$ was placed on a glass slide to obtain the corresponding Raman fingerprint, which was observed with a high signal-to-noise ratio. The Raman spectrum of **R-1**$_{Agg}$ shows two peaks at 1584 cm^{-1} (strong, C–C aromatic ring chain vibrations) and 1180–1208 cm^{-1} (weak, C–O–C asymmetric vibrations). Furthermore, the droplets examined after purging the

Fig. 4 (a) Raman spectra of **R-1**$_{Agg}$ (4×10^{-4} M) in aqueous medium (water/THF, 99/1 v/v) and after purging with CO_2. (b) SERS spectra of **R-1**$_{Agg}$ in the presence of Au-NPs (1/9 v/v) and after purging with CO_2.

aggregate solution with CO_2 showed a reduction in the peak intensity to almost baseline; thus, by monitoring the Raman-active peaks of **R-1**$_{Agg}$, it was possible to detect CO_2 gas (Fig. 4a).

Along with the inherent AERS phenomenon, we also looked for surface-enhanced Raman scattering (SERS) due to its enhanced sensitivity compared to normal Raman scattering. The Raman spectrum of **R-1**$_{Agg}$ was recorded using spherical gold nanoparticles (Au-NPs) as the SERS substrate. **R-1**$_{Agg}$ was mixed with as-prepared Au-NPs (size *ca.* 40 nm) in 1 : 9 ratio (v/v), and the mixture was incubated for 10 min to obtain maximum adsorption. The SERS spectra were recorded as described above, and *ca.* 25-fold enhancement in the intensity was observed when compared with normal Raman intensity obtained for **R-1**$_{Agg}$ (Fig. 4). In comparison to the spectrum obtained from AERS, the SERS-assisted spectrum showed well-resolved peaks along with a unique signal at 2213 cm^{-1} resulting from the –CN group, which can be monitored easily for the CO_2 sensing experiment.

In conclusion, the cyano-substituted *p*-phenylenevinylene derivative **R-1** reported in this study underwent aggregation in an aqueous medium, exhibiting AIE and AERS phenomena, which were used for the detection of CO_2 gas among different specimens of neutral gases. The AIE-based CO_2 assay described here is useful for detecting CO_2 in biological specimens. The novelty of the present system is that a combination of fluorescence and AERS or SERS can be used for sensing CO_2. However, for ratiometric sensing and *in vivo* applications, further improvement over the present design is required and such studies are in progress.

Conflicts of interest

There are no conflicts to declare.

Notes and references

1 (*a*) F. A. Rahman, M. M. A. Aziz, R. Saidur, W. A. W. A. Bakar, M. R. Hainin, R. Putrajaya and N. A. Hassan, *Renewable Sustainable Energy Rev.*, 2017, **71**, 112–126; (*b*) T. R. Anderson, E. Hawkins and P. D. Jones, *Endeavour*, 2016, **40**, 178–187; (*c*) D. M. D'Alessandro, B. Smit and J. R. Long, *Angew. Chem., Int. Ed.*, 2010, **49**, 6058–6082.
2 (*a*) S. Zeng, X. Zhang, L. Bai, X. Zhang, H. Wang, J. Wang, D. Bao, M. Li, X. Liu and S. Zhang, *Chem. Rev.*, 2017, **117**, 9625–9673; (*b*) H. Liu, S. Lin, Y. Feng and P. Theato, *Polym. Chem.*, 2017, **8**, 12–23; (*c*) A. Darabi, P. G. Jessop and M. F. Cunningham, *Chem. Soc. Rev.*, 2016, **45**, 4391–4436; (*d*) P. G. Jessop, S. M. Mercera and D. J. Heldebrant, *Energy Environ. Sci.*, 2012, **5**, 7240–7253; (*e*) T. Yu, R. Cristiano and R. G. Weiss, *Chem. Soc. Rev.*, 2010, **39**, 1435–1447; (*f*) D. M. Rudkevich and H. Xu, *Chem. Commun.*, 2005, 2651–2659.
3 X. Zhou, S. Lee, Z. Xu and J. Yoon, *Chem. Rev.*, 2015, **115**, 7944–8000.
4 (*a*) Y. Ma, M. Cametti, Z. Džolić and S. Jiang, *J. Mater. Chem. C*, 2018, **6**, 9232–9237; (*b*) D. S. Philips, S. Ghosh, K. V. Sudheesh, C. H. Suresh and A. Ajayaghosh, *Chem. – Eur. J.*, 2017, **23**, 17973–17980; (*c*) X. Zhang, S. Lee, Y. Liu, M. Lee, J. Yin, J. L. Sessler and J. Yoon, *Sci. Rep.*, 2014, **4**, 4593; (*d*) W. Hong, Y. Chen, X. Feng, Y. Yan, X. Hu, B. Zhao, F. Zhang, D. Zhang, Z. Xu and Y. Lai, *Chem. Commun.*, 2013,
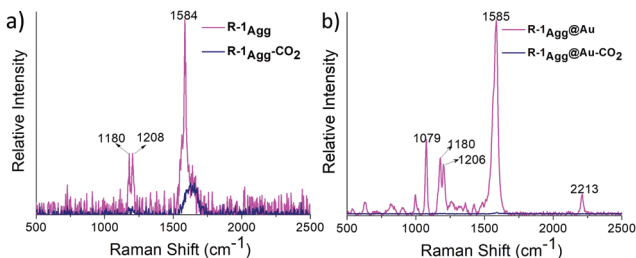
49, 8229–8231; (*e*) T. Tian, X. Chen, H. Li, Y. Wang, L. Guo and L. Jiang, *Analyst*, 2013, **138**, 991–994; (*f*) Q. Xu, S. Lee, Y. Cho, M. H. Kim, J. Bouffard and J. Yoon, *J. Am. Chem. Soc.*, 2013, **135**, 17751–17754; (*g*) M. Ishida, P. Kim, J. Choi, J. Yoon, D. Kim and J. L. Sessler, *Chem. Commun.*, 2013, **49**, 6950–6952; (*h*) L. Q. Xu, B. Zhang, M. Sun, L. Hong, K.-G. Neoh, E.-T. Kang and G. D. Fu, *J. Mater. Chem. A*, 2013, **1**, 1207–1212.

5 (*a*) Z. Guo, N. R. Song, J. H. Moon, M. Kim, E. J. Jun, J. Choi, J. Y. Lee, C. W. Bielawski, J. L. Sessler and J. Yoon, *J. Am. Chem. Soc.*, 2012, **134**, 17846–17849; (*b*) R. Ali, T. Lang, S. M. Saleh, R. J. Meier and O. S. Wolfbeis, *Anal. Chem.*, 2011, **83**, 2846–2851; (*c*) Y. Liu, Y. Tang, N. N. Barashkov, I. S. Irgibaeva, J. W. Y. Lam, R. Hu, D. Birimzhanova, Y. Yu and B. Z. Tang, *J. Am. Chem. Soc.*, 2010, **132**, 13951–13953; (*d*) T. Gunnlaugsson, P. E. Kruger, P. Jensen, F. M. Pfeffer and G. M. Hussey, *Tetrahedron Lett.*, 2003, **44**, 8909–8913; (*e*) E. M. Hampe and D. M. Rudkevich, *Chem. Commun.*, 2002, 1450–1451.

6 (*a*) P. Anees, V. K. Praveen, K. K. Kartha and A. Ajayaghosh, *Comprehensive Supramolecular Chemistry II*, Elsevier, 2017, pp. 297–320; (*b*) D. Zhai, W. Xu, L. Zhang and Y.-T. Chang, *Chem. Soc. Rev.*, 2014, **43**, 2402–2411.

7 (*a*) M. M. Joseph, N. Narayanan, J. B. Nair, V. Karunakaran, A. N. Ramya, P. T. Sujai, G. Saranya, J. S. Arya, V. M. Vijayan and K. K. Maiti, *Biomaterials*, 2018, **181**, 140–181; (*b*) D. L. Akins, *Nanomater. Nanotechnol.*, 2014, **4**, DOI: 10.5772/58403.

8 (*a*) M. Martínez-Abadía, R. Giménez and M. B. Ros, *Adv. Mater.*, 2018, **30**, 1704161; (*b*) T. Noguchi, B. Roy, D. Yoshihara, J. Sakamoto, T. Yamamoto and S. Shinkai, *Angew. Chem., Int. Ed.*, 2016, **128**,

5802–5806; (*c*) F. Aparicio, S. Cherumukkil, A. Ajayaghosh and L. Sánchez, *Langmuir*, 2016, **32**, 284–289; (*d*) L. Zhu and Y. Zhao, *J. Mater. Chem. C*, 2013, **1**, 1059–1065; (*e*) B.-k. An, J. Gierschner and S. Y. Park, *Acc. Chem. Res.*, 2012, **45**, 544–554.

9 (*a*) S. Yagai, S. Okamura, Y. Nakano, M. Yamauchi, K. Kishikawa, T. Karatsu, A. Kitamura, A. Ueno, D. Kuzuhara, H. Yamada, T. Seki and H. Ito, *Nat. Commun.*, 2014, **5**, 4013; (*b*) V. K. Praveen, C. Ranjith, E. Bandini, A. Ajayaghosh and N. Armaroli, *Chem. Soc. Rev.*, 2014, **43**, 4222–4242; (*c*) L. Maggini and D. Bonifazi, *Chem. Soc. Rev.*, 2012, **41**, 211–241; (*d*) A. Ajayaghosh and V. K. Praveen, *Acc. Chem. Res.*, 2007, **40**, 644–656.

10 (*a*) J. Mei, N. L. C. Leung, R. T. K. Kwok, J. W. Y. Lam and B. Z. Tang, *Chem. Rev.*, 2015, **115**, 11718–11940; (*b*) X. Ma, R. Sun, J. Cheng, J. Liu, F. Gou, H. Xiang and X. Zhou, *J. Chem. Educ.*, 2016, **93**, 345–350.

11 (*a*) S.-J. Yoon, J. W. Chung, J. Gierschner, K. S. Kim, M.-G. Choi, D. Kim and S. Y. Park, *J. Am. Chem. Soc.*, 2010, **132**, 13675–13683; (*b*) S. S. Babu, V. K. Praveen, S. Prasanthkumar and A. Ajayaghosh, *Chem. – Eur. J.*, 2008, **14**, 9577–9584; (*c*) J. Gierschner, M. Ehni, H.-J. Egelhaaf, B. Milián-Medina, D. Beljonne, H. Benmansour and G. C. Bazan, *J. Chem. Phys.*, 2005, **123**, 144914.

12 (*a*) P. D. Vaidya and E. Y. Kenig, *Chem. Eng. Technol.*, 2007, **30**, 1467–1474; (*b*) M. Caplow, *J. Am. Chem. Soc.*, 1968, **90**, 6795–6803.

13 (*a*) N. Narayanan, V. Karunakaran, W. Paul, K. Venugopal, K. Sujathan and K. K. Maiti, *Biosens. Bioelectron.*, 2015, **70**, 145–152; (*b*) A. N. Ramya, A. Samanta, N. Nisha, Y. T. Chang and K. K. Maiti, *Nanomedicine*, 2015, **10**, 561–571.